

# **PROPELLER INDUCED STRUCTURAL VIBRATION THROUGH THE THRUST BEARING**

**Jie Pan, Nabil Farag, Terry Lin and Ross Juniper\***

DEPARTMENT OF MECHANICAL AND MATERIALS ENGINEERING  
THE UNIVERSITY OF WESTERN AUSTRALIA  
35 STIRLING HIGHWAY, CRAWLEY, WA 6009, AUSTRALIA

\*MARITIME PLATFORMS DIVISION  
AERONAUTICAL & MARITIME RESEARCH LABORATORY  
CORDITE AVENUE, MARIBYRNONG 3032, VIC. AUSTRALIA

## **ABSTRACT**

Propeller induced structural vibration through the thrust bearing is an important source for low frequency shipboard noise and underwater sound radiation from a submarine hull. Such vibration is investigated using a scaled experimental model. This research concentrates on the experimental characterization of propeller force, hydrodynamic force of the thrust bearing and vibration transmission through a thrust bearing into the supporting structure. The results of laboratory measurement of the propeller force and the complex hydrodynamic stiffness of the thrust bearing are presented in this paper. The response of the shaft axial vibration and flexural vibration of the supporting structure is also analyzed.

## **I. INTRODUCTION**

While the propeller delivers thrust to submarines and surface ships, it also generates oscillatory disturbances. A particular disturbance, as the focus of this paper, is due to the asymmetry in the hull or protrusions of control surfaces or shaft bearing struts, which results in a non-uniform wake velocity in the fluid field near the propeller. A small variation of thrust is then produced when the blades rotate through the non-uniform wake. The frequency of this variation is well known as the blade passing frequency, which is equal to the shaft rotational speed multiplied by the number of blades on the propeller.

The oscillatory thrust axially acting on the shaft generates ship structural vibration through the hydrodynamic stiffness force of the lubricant oil film between the tilting pads and the shaft collar.

One option for reducing the propeller induced ship structural vibration is to actively decrease the hydrodynamic stiffness at the frequencies of the oscillatory thrust by introducing a negative spring stiffness using magnetic actuators [1]. With a minimum hydrodynamic stiffness, the

transmission of the oscillatory stiffness force through the oil film can be minimised. This “control at the source” indicates new promise in reducing propeller-induced vibration.

Effective control of propeller induced vibration at the thrust bearing requires a clear understanding of the hydrodynamic stiffness of the lubricant oil film. A literature survey suggested that hydrodynamic stiffness of the fluid film is related to thrust (steady load), and shaft speed [2] among other factors. The dependence of the stiffness on the frequency and shaft speed is nonlinear. The complex nonlinear dynamics of the thrust bearing increases the difficulty for active control of the hydrodynamic stiffness. Traditional linear control design methods is no longer suitable for such nonlinear system in hand. The understanding of nonlinear system dynamics is vital for the stability analysis, robustness and design of control laws. It is also related to the selection of control actuators.

Work described in this paper is a preliminary investigation into the vibration transmission characteristics of the thrust bearing. It includes the laboratory determination of propeller oscillatory thrust and hydrodynamic force of the lubricant oil film in the thrust bearing. The shaft and supporting structure response to the thrust excitation is also analysed.

## II. DESCRIPTION OF DYNAMIC SYSTEM

A generic propeller shaft system is outlined in Figure 1. It represents a typical propeller shaft system in the main propulsion unit in marine installations. The system consists of the propeller, propeller shaft, thrust bearing and part of the flexible coupling in the propeller side. It has been shown in a previous report [3] that the flexible coupling isolates the engine side from the propeller side of the propulsion system, as far as the axial vibration is concerned. This eliminates the effect of engine excitation on the supporting structure of the thrust bearing.

A three-blade propeller with a diameter of  $0.2m$  is attached to one end of the propeller shaft and placed in a water tank ( $0.99 \times 0.585 \times 0.58m^3$ ) as shown in Figure 2. Two journal bearings are used to support the shaft. They are respectively located on the tank wall and on the supporting structure. The 8-pad fixed taper thrust bearing is designed according to reference [4] to allow the establishment of hydrodynamic lubrication between the runner and thrust pads.

A circular shoulder is fixed to the propeller shaft, where the shaft can be excited by an impact hammer and the shaft axial motion can be measured by a linear laser vibrometer and inductive displacement pickup. The thrust bearing is supported by a steel plate ( $1 \times 0.6 \times 0.0016m^3$ ) clamped to an angle steel frame. Accelerometers are attached to the bearing housing and supporting structure for measuring the system response.

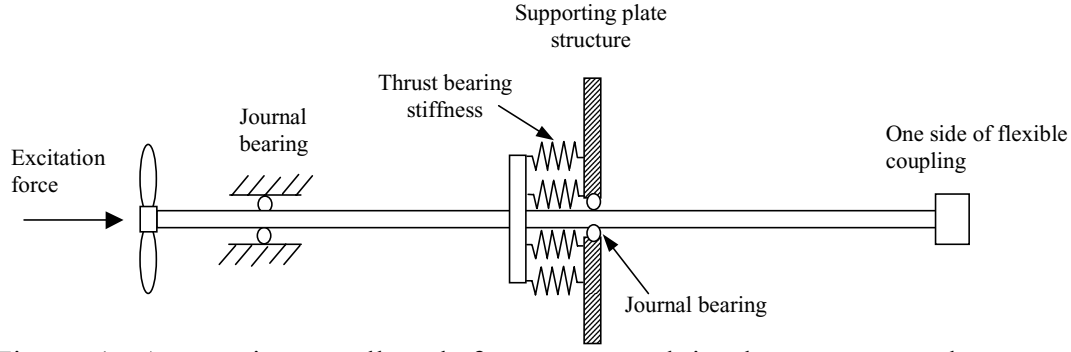


Figure 1: A generic propeller shaft system used in the present study to represent real installation in marine applications.

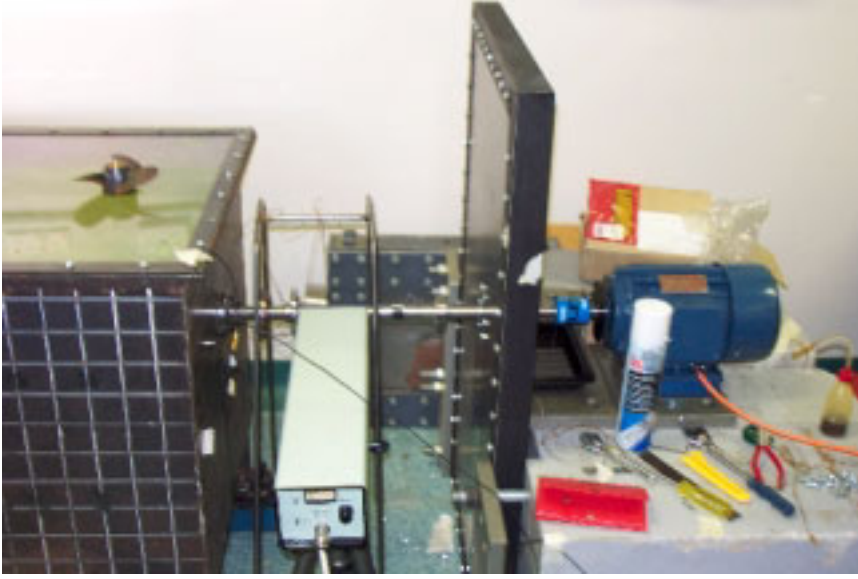


Figure 2: A photo of the test rig.

### III. MEASUREMENT OF PROPELLER DYNAMIC THRUST

The propeller thrust plays a dominant role in exciting the vibration of the shaft and supporting structure. It also directly affects the characteristics of the hydrodynamic stiffness of the thrust bearing. In this paper, we propose an experimental method to determine the propeller force *in situ* using the mobility measurements.

Propeller shaft response  $v$  is related to the input mobility function  $M_{ss}$  and excitation force  $F$  by:

$$v = M_{ss} F. \quad (1)$$

At low frequencies, the shaft can be approximated as a rigid mass. Thus the input mobility function is independent of the excitation location on the shaft. We used the impact method to measure the mobility function of the shaft at different engine speeds. An impact force is applied at the circular shoulder and the axial velocity of the shaft is also measured at the shoulder. For such measurement, the shaft response is due to propeller force and impact hammer force and the latter is removed by

$$v_I = v_{I+P} - v_P \quad (2)$$

where  $v_I$  and  $v_P$  are the shaft velocity response due to hammer and propeller excitation respectively.  $v_{I+P}$  is the response to the combined excitation of the hammer and propeller.

Equation (2) is implemented in the frequency domain. Results from 10 measurements are averaged to minimize the variation due to the phase differences between the two excitations and the effect of other disturbances. The mobility function of the shaft is then calculated from  $v_I$  and the measured impact force  $F_I$  at different engine speeds:

$$M_{ss} = \frac{v_I}{F_I}. \quad (3)$$

Thus the direct result from this measurement is the propeller dynamic thrust  $F_p$ :

$$F_p = \frac{v_p}{M_{ss}}. \quad (4)$$

In the meantime, the effect of the engine speed on the mobility function can be related to the characteristics of the hydrodynamic force at the thrust bearing.

Figure 3 is the waterfall plot of the shaft longitudinal vibration velocity measured on the shaft shoulder by a laser velocity transducer at different rotational speeds. The shaft response is mainly at the blade passing frequency and at the rotating frequency of the shaft. The response at the latter frequency is due to the dynamic characteristics of the propeller shaft itself such as misalignment.

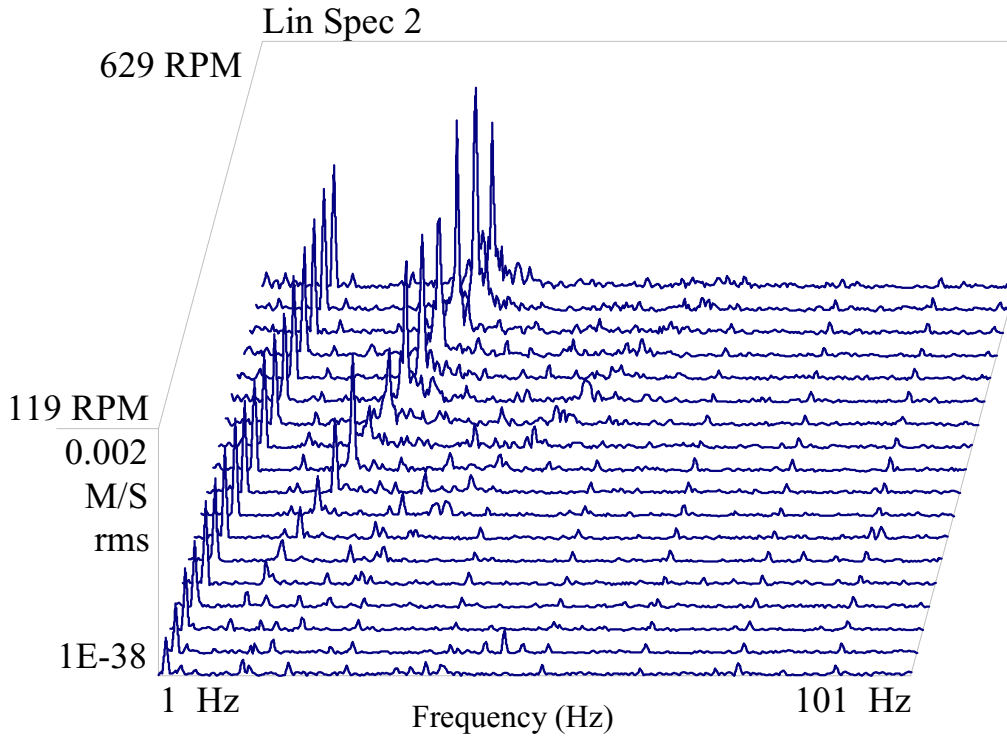


Figure 3: Shaft axial vibration velocity at different shaft speeds.

Concentrating at the blade passing frequency, we were able to obtain the propeller dynamic thrust at this frequency and at different shaft speeds as shown in Figure 4. This measurement provides the thrust magnitudes at each shaft speed. The overall trend agrees with the existing understanding of the square functional relationship between the propeller force and shaft rotating speed  $\omega_s$ :

$$F_p \propto \omega_s^2 \quad (5)$$

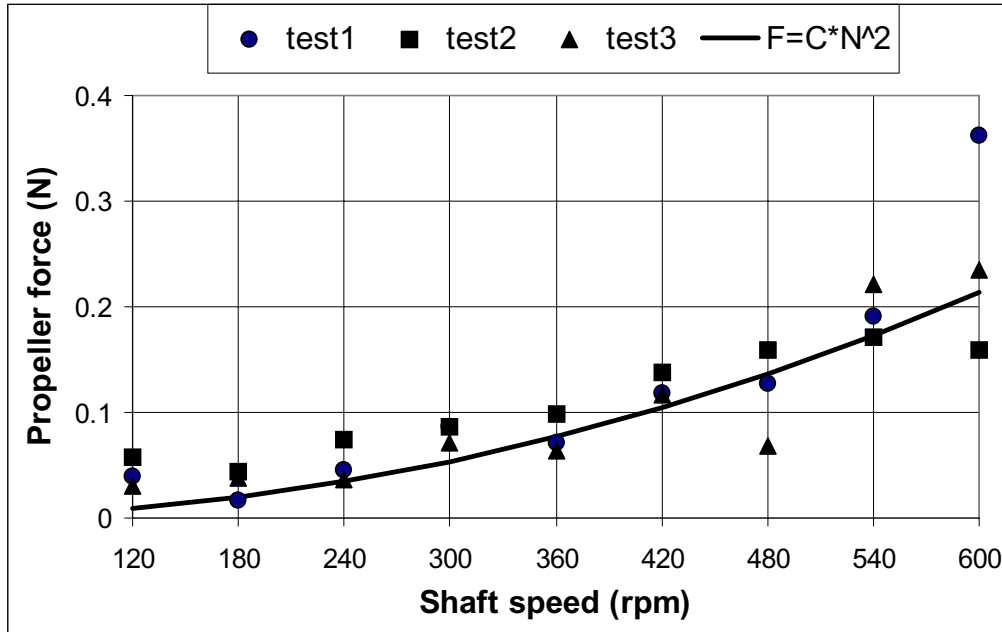


Figure 4: Propeller dynamic thrust at blade passing frequency and at different shaft speeds.

It is observed from Figure 3 that the shaft response at the blade passing frequency does not follow the square relationship with the shaft speed as the thrust does. This observation suggests that the mobility function at the blade passing frequency is not a constant. A straightforward explanation is that the propeller shaft response is controlled by the resonance of the system including propeller, shaft, thrust bearing, and supporting structure. When the blade passing frequency is close to the resonance frequency of the system, an increase in the shaft velocity response is observed. Indeed the measured mobility function (Figure 5) shows two resonance peaks in the low frequency range ( $<37\text{Hz}$ ). Furthermore the resonance frequency and the peak value in the mobility function vary with the shaft speed.

Such variation in mobility function characteristics may be linked with the variation of the hydrodynamic stiffness and damping of the thrust bearing.

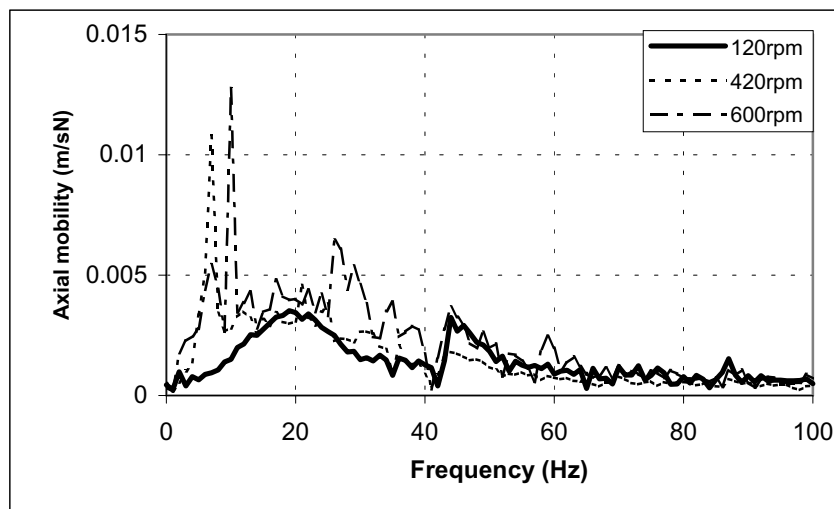


Figure 5: Measured mobility functions of the shaft system at different shaft speeds.

#### IV. MEASUREMENT OF HYDRODYNAMIC FORCE OF THRUST BEARING

The hydrodynamic force includes the stiffness and viscous forces of the lubricant oil film in the thrust bearing. It is the constraint force for the characteristics of the shaft vibration. It is the excitation force that directly drives the supporting structure at the thrust bearing housing. A simple two-degree of freedom model of the propeller shaft, thrust bearing and supporting plate is shown in Figure 6. In this model, we assume that the only unknown parameters are the stiffness and damping of the thrust bearing. As a result, the force balance equation for the shaft mass motion is

$$m_s \ddot{x}_s + k_H \Delta x + c_H \dot{\Delta x} + k_s x_s + c_s \dot{x}_s = F_p + F_I \quad (6)$$

where  $m_s$  is the mass of propeller shaft including propeller, shaft and hydrodynamic inertia (add mass).  $k_s$  and  $c_s$  are the stiffness and damping coefficients from those constraint forces at the propeller and journal bearings.  $\Delta x = x_s - x_p$  is the relative displacement between the shaft and thrust bearing housing. The hydrodynamic force (stiffness and damping) of the thrust bearing is described by a complex stiffness in the frequency domain:

$$\bar{k}_H(\omega) = k_H(\omega) + j\omega c_H(\omega). \quad (7)$$

By expressing the hydrodynamic force of the thrust bearing in the form of Equation (7), we have restricted the validity of our method to the linearized range of  $|\Delta x| = \Delta_o$  where  $\Delta_o$  is the amplitude of  $\Delta x$ . Nevertheless, this model allows nonlinear dependence of  $k_H$  and  $c_H$  on  $\Delta x$ .

Dividing the forcing term on the both sides of equation (6) in the frequency domain, we then obtained following expression for the determination of the complex stiffness of the thrust bearing;

$$\bar{k}_H(\omega) = \frac{j\omega[1 - jm_s\omega M_{ss}] - (k_s + j\omega c_s)M_{ss}}{[M_{ss} - M_{ps}]} \quad (8)$$

where  $M_{sp}$  is the mobility function of the system with impact force on the shaft and response measured on the thrust bearing housing.

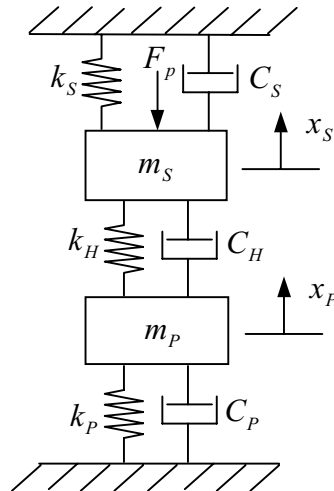


Figure 6: A two degree of freedom model representing the propeller shaft, thrust bearing and supporting plate.

Figure 7 shows the magnitude of the complex stiffness of the thrust bearing at three different shaft speeds. An interesting observation of Figure 7 is the dependence of the complex stiffness upon the shaft speeds. The difference between the thrust bearing complex stiffness at different speeds is evident at low frequencies. At low frequencies, the lubricant film is in the stiffness controlled region. Therefore the observable difference actually demonstrates the change of the hydrodynamic stiffness of lubricant film with shaft speed. The frequency dependence of the complex stiffness requires further investigation by separating the stiffness and viscous damping terms.

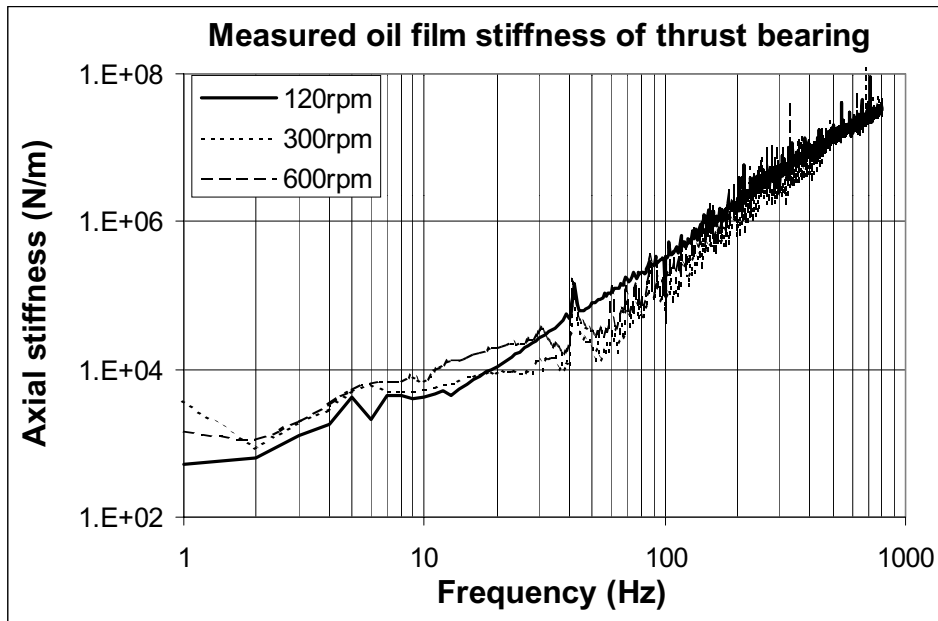


Figure 7: Magnitude of the complex stiffness of the thrust bearing at two different shaft speeds.

## V. SYSTEM RESPONSE

As a preliminary study, a constant stiffness of the thrust bearing at the low frequency ( $6 \times 10^4 (N/m)$ ) is used for the prediction of the axial mobility function of the propeller shaft. The mass and stiffness of the supporting structure are included in the prediction using Finite Element Analysis. Figure 8 is the measured and predicted axial input mobility function of the shaft when the shaft speed is at 600rpm.

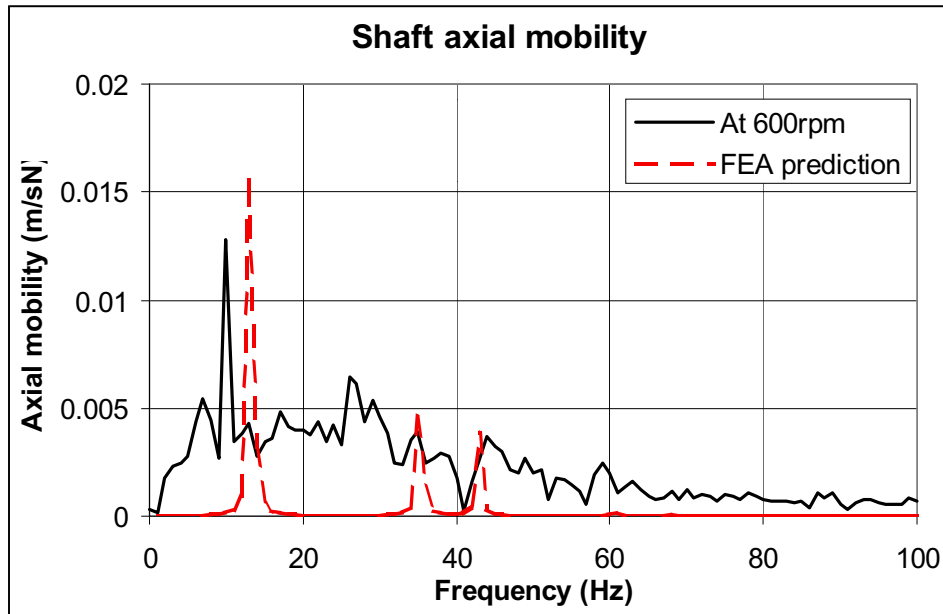


Figure 8: Propeller shaft input mobility function at 600rpm.

The mode shapes corresponding to the three resonance peaks are shown in Figure 9. The coupling between the plate distributed mode and the shaft rigid body modes is demonstrated there.

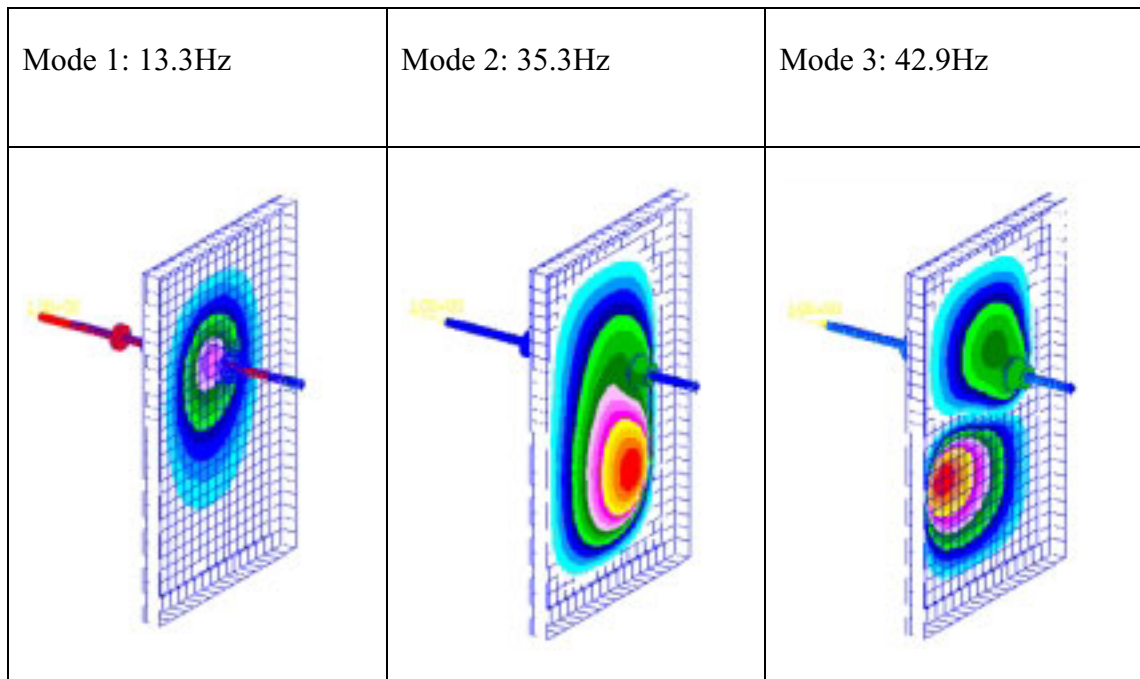


Figure 9. The mode shapes corresponding to the three resonant peaks in the mobility function.

The measured response of the supporting plate at (105mm,250mm) from the upper-right corner is shown in the waterfall plot in Figure 10 as a function of shaft speed. As expected, the peak



responses at the blade passing frequency and at the shaft frequency are identifiable. The magnitude variation at those frequencies indicates the effect of the system resonance and modal response of the plate vibration.

## VI. CONCLUSIONS

This paper focuses on the understanding of structural vibration excited by propeller dynamic thrust along the shaft. The measurement of the shaft axial mobility function allows the experimental determination of the propeller force at the blade passing frequency. It was found that the mobility function is characterized by resonance peaks at low frequencies. The variation of the resonance frequencies of the propeller shaft with shaft speed demonstrates the significant effect of the hydrodynamic stiffness of the thrust bearing on the system characteristics.

This paper also presents an approximate experimental method to measure the complex hydrodynamic stiffness of the thrust bearing. A significant change of the complex stiffness in the stiffness controlled frequency range with shaft speed is observed. This observation and experimental method may lead to a better understanding of the dynamics of thrust bearing for potential active control of the hydrodynamic force transmission into the supporting structure. For active control of a nonlinear system in particular, the effective cancellation of the nonlinear stiffness force at the thrust bearing requires an accurate model of such stiffness and methods to determine it on line.

The paper also covers the analysis of the system response (shaft and supporting panel) to the propeller force and the hydrodynamics of the thrust bearing. The mode shapes of the coupled shaft-plate system are obtained by FEA and provide useful insight for the system vibration analysis.

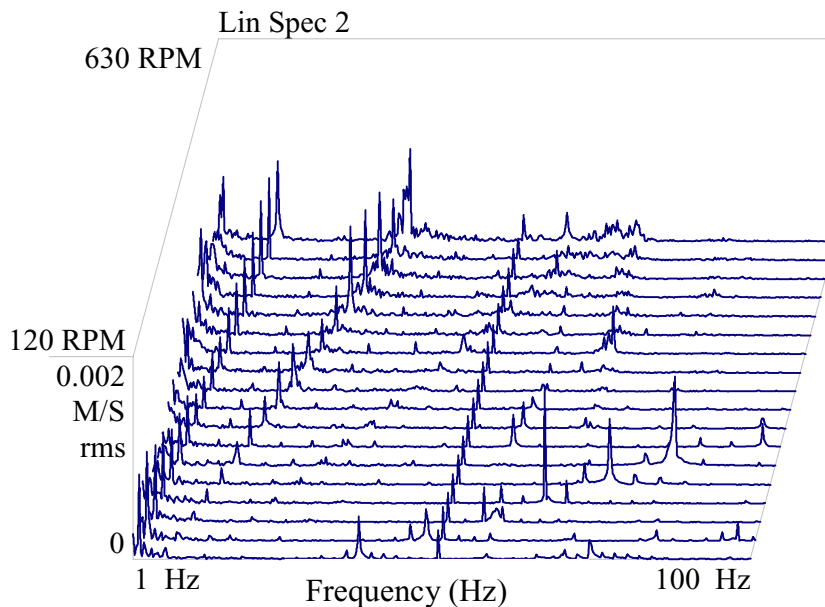


Figure 10. Measured response of the supporting plate at different shaft speeds.

## **ACKNOWLEDGMENTS**

Support for this work from the Defense Science and Technology Organization is gratefully acknowledged.

## **REFERENCES**

- [1] Lewis, D.W. and Allaire, P.E., “Active magnetic control of oscillatory axial shaft vibrations in ship shaft transmission systems, Part 1: System natural frequencies and laboratory scale model”, *Journal of Tribology Transactions*, 32, 170-178, (1989).
- [2] Parkins, D. W. and Horner, D., “Tilting pad journal bearing --- measured and predicted stiffness coefficients”, *Journal of Tribology Transactions*, 36, 359-366, (1993).
- [3] Pan, J., Lin, T. and Farag, N., “Characterisation and control of thrust bearing vibration” Issue 2, April 2002, report to DSTO.
- [4] Neale M. J., “The Tribology Handbook”, Butterworth-Heinemann Ltd., Oxford, Great Britain (1995).